Interaction of a uniform current with a cylinder submerged beneath a defective ice sheet

Yifeng Yang[1], **G.X. Wu**[1]
[1]Department of Mechanical Engineering, University College London, London, UK.
E-mail Address of the presenting author: yifeng.yang.19@ucl.ac.uk

1 INTRODUCTION

Problems involving fluid–structure–ice interaction are of significant importance in polar engineering. One of the key concerns is how a current interacts with underwater obstacles, which is related to ice breaking by submerged vehicles [1]. A series of research has been undertaken on this topic. Particularly, Savin & Savin [2] modelled a submerged circular cylinder as a dipole and its strength was taken as that in the unbounded fluid domain. Sturova [3] solved the problem of a sphere advancing at a constant speed by employing a multipole expansion method. Li et al. [4] further solved the problem of a current interaction with a circular cylinder beneath a perfect ice sheet without the approximation in [2]. Yang et al. [5] considered the problem of a circular cylinder submerged below a free surface covered by a semi-infinite ice sheet using Weiner-Hopf method. More recently, Yang & Wu [6] developed a method for the solution at the critical speeds. All these works are for a perfect ice sheet. Here, we shall consider a current passing a cylinder submerged below an ice sheet with a defect or an internal physical constraint.

2 BOUNDARY VALUE PROBLEM AND SOLUTION PROCEDURE

The problem of a uniform current interaction with a cylinder submerged beneath a defective ice sheet is sketched in Figure. 1. A Cartesian coordinate system O-xz is defined, with x-axis along the undisturbed mean water surface, and z-axis points vertically upwards. The water surface is covered by a homogeneous ice sheet of thickness h, which is subjected to a defect at $x = 0$. A uniform current with speed U that comes from $x = +\infty$ will be disturbed by a submerged cylinder.

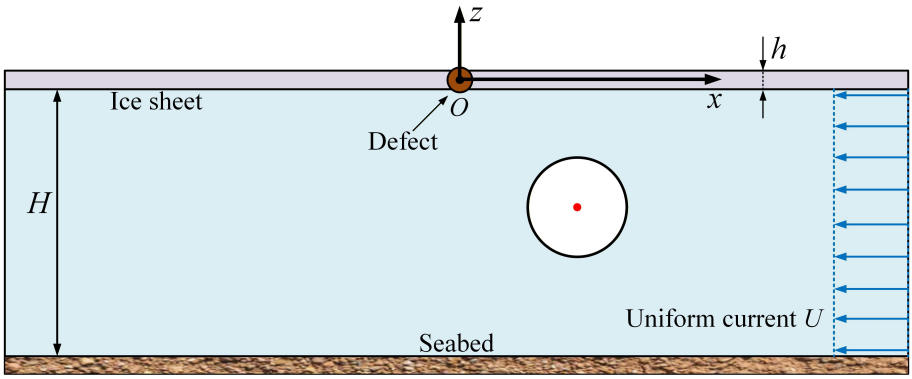

Figure. 1. Sketch of the problem and the coordinate system.

The fluid with density ρ and mean water depth H is assumed to be inviscid, incompressible and homogeneous, and its motion is irrotational. It is further assumed that the disturbed wave amplitude is small compared with the wavelength. Hence, the linearised velocity potential theory is employed to describe the problem. The total velocity potential can be written as

$$\Phi(x,z) = -Ux + \phi(x,z), \quad -\infty < x < +\infty, \qquad -H \le z \le 0. \tag{1}$$

where ϕ denotes the disturbed velocity potential, and is governed by the Laplace equation, or

$$\nabla^2\phi(x,z)=0, \qquad -\infty<x<+\infty, \qquad -H\le z\le 0. \tag{2}$$

The kinematic and dynamic boundary conditions on the ice sheet provide

$$-U\frac{\partial\eta}{\partial x}=\frac{\partial\phi}{\partial z}, \qquad z=0, \tag{3}$$

$$\left(L\frac{\partial^4}{\partial x^4}+\rho g\right)\eta=\rho U\frac{\partial\phi}{\partial x}, \qquad z=0, \tag{4}$$

where η denotes the ice sheet deflection, L represents the flexural rigidity of the ice sheet, and g is the acceleration due to gravity. On the body surface and the seabed, the impermeable conditions are imposed as

$$\frac{\partial\phi}{\partial n}=Un_x, \qquad \text{on } S_B, \tag{5}$$

$$\frac{\partial\phi}{\partial z}=0, \qquad z=-H, \tag{6}$$

where $\boldsymbol{n}=(n_x,n_z)$ denotes the unit normal vector of S_B. At $x=0$, a defect is assumed in the ice sheet and represented as a physical constraint. Three types of physical constraints are considered, and the corresponding edge conditions are imposed as [7]

$$\begin{cases} \eta=\dfrac{\partial\eta}{\partial x}=0 & \text{Clamped} \\ \eta=\dfrac{\partial^2\eta}{\partial x^2}=0 & \text{Simply supported,} \\ \dfrac{\partial^2\eta}{\partial x^2}=\dfrac{\partial^3\eta}{\partial x^3}=0 & \text{Free} \end{cases} \qquad x=0^{\pm} \text{ and } z=0. \tag{7}$$

At infinity, the far-field radiation condition is imposed. Consequently, waves propagating towards $x=+\infty$ and $x=-\infty$ have group velocities greater and less than U respectively.

To solve the boundary value problem above, we may use the Green function G satisfying all boundary conditions, apart from those at $x=0$ and on S_B, which can be written as [4]

$$G=\ln\left(\frac{r_1}{H}\right)+\ln\left(\frac{r_2}{H}\right)-\int_{-\infty}^{+\infty}\frac{e^{-|\alpha|H}\left(L\alpha^4+\rho g+\rho U^2|\alpha|\right)C(z,\alpha)C(z_0,\alpha)e^{-\mathrm{i}\alpha(x-x_0)}}{K(\alpha,U)}\mathrm{d}\alpha, \tag{8}$$

where $r_1=\sqrt{(x-x_0)^2+(z-z_0)^2}$, $r_2=\sqrt{(x-x_0)^2+(z+z_0+2H)^2}$,

$$C(z,\alpha)=\cosh\alpha(z+H), \tag{9}$$

$$K(\alpha,U)=(L\alpha^4+\rho g)\alpha\sinh(\alpha H)-\rho U^2\alpha^2\cosh(\alpha H). \tag{10}$$

In Eq. (8), there will be poles in the integrand at $K(\alpha,U)=0$. Particularly, the second-order pole at $\alpha=0$ is treated using the Hadamard regularisation and the Cauchy principal value. $K(\alpha,U)=0$ may also have non-zero real roots which are related to the water depth-based Froude number $F=U/\sqrt{gH}$. The nature of these roots and integration paths at the roots have been discussed in detail in [5]. With the help of G, ϕ can be converted into an integral equation over S_B, and additional contributions arising at $x_0=0$, obtained from integration by parts on the ice sheet

$$2\pi\phi(x,z)=\int_{S_B}\left[\phi(x_0,z_0)\frac{\partial G(x,z;x_0,z_0)}{\partial n_0}-G(x,z;x_0,z_0)\frac{\partial\phi(x_0,z_0)}{\partial n_0}\right]\mathrm{d}s_0+A_j\frac{\partial^j\xi(x,z;0)}{\partial x^j}$$
$$+A_k\left[\frac{\partial^k\xi(x,z;0)}{\partial x^k}+\delta_{k3}\frac{\rho U}{L}G(x,z;0,0)\right], \tag{11}$$

where $(j,k)=(0,1)$, $(0,2)$ and $(2,3)$ correspond to clamped, simply supported and free edges respectively, δ_{ij} denotes the Kronecker delta function. A_j and A_k are unknowns related to the jumps of physical parameters at the constraint, or

$$A_j=\frac{L}{\rho}\left[\frac{\partial^{3-j}\eta(x_0)}{\partial x_0^{3-j}}\right]_{x_0=0^+}^{x_0=0^-}, \qquad A_k=\frac{L}{\rho}\left[\frac{\partial^{3-k}\eta(x_0)}{\partial x_0^{3-k}}\right]_{x_0=0^+}^{x_0=0^-}. \tag{12a, b}$$

$$\xi(x,z;x_0)=\left[\frac{L}{\rho gU}\frac{\partial^4G(x,z;x_0,z_0)}{\partial x_0^3\partial z_0}+\frac{U}{g}\frac{\partial G(x,z;x_0,z_0)}{\partial x_0}\right]_{z_0=0}=-\mathrm{i}\rho U\int_{-\infty}^{+\infty}\frac{\alpha C(z,\alpha)e^{-\mathrm{i}\alpha(x-x_0)}}{K(\alpha,U)}\mathrm{d}\alpha \tag{13}$$

which gives $\xi_x(x,z;x_0) = -\xi_{x_0}(x,z;x_0)$ used in Eq. (11). For clamped and simply supported edges, Eq. (11) shows that they are mathematically equivalent to placing a dipole and two multipoles of different orders at the constraint, and the strength of the dipole and that of one multipole are related. In the free edge case, a source is being placed together with three multipoles of different orders. The strengths of two multipoles are related, and strength of the source is linked to that of the other multipole. Due to the source term, there is an equal and opposite flux in the far field [6], the difference of which is equal to the flux due to the jump of the ice sheet deflection at the constraint, or $U[\eta(x)]_{x=0^+}^{x=0^-}$ as shown in Eq.(3). Applying Eq. (13) to Eq. (11), the equation for ice sheet deflection $\eta(x)$ provides

$$2\pi\eta(x) = -\int_{S_B}\left[\phi(x_0,z_0)\frac{\partial\xi(x,z_0;x_0)}{\partial n_0} - \xi(x,z_0;x_0)\frac{\partial\phi(x_0,z_0)}{\partial n_0}\right]\mathrm{d}s_0 + A_j\frac{\mathrm{d}^j I(x)}{\mathrm{d}x^j} + A_k\left[\frac{\mathrm{d}^k I(x)}{\mathrm{d}x^k} - \delta_{k3}\frac{\rho U}{L}\xi(x,0;0)\right], \tag{14}$$

where

$$I(x) = \left[\frac{L}{\rho g U}\frac{\partial^4\xi(x,z;0)}{\partial x^3\partial z} + \frac{U}{g}\frac{\partial\xi(x,z;0)}{\partial x}\right]_{z=0} = -\rho\int_{-\infty}^{+\infty}\frac{\alpha\sinh(\alpha H)}{K(\alpha,U)}e^{-\mathrm{i}\alpha x}\mathrm{d}\alpha. \tag{15}$$

To solve A_j and A_k, we may substitute Eq. (14) into the edge condition in Eq. (7), we have

$$\begin{cases}\dfrac{\mathrm{d}^{2j}I(x)}{\mathrm{d}x^{2j}}A_j + \left[\dfrac{\mathrm{d}^{j+k}I(x)}{\mathrm{d}x^{j+k}} - \delta_{k3}\dfrac{\rho U}{L}\dfrac{\partial^j\xi(x,0;0)}{\partial x^j}\right]A_k = \displaystyle\int_{S_B}\left[\phi\frac{\partial^{j+1}\xi}{\partial x^j\partial n_0} - \frac{\partial^j\xi}{\partial x^j}\frac{\partial\phi}{\partial n_0}\right]\mathrm{d}s_0 \\ \dfrac{\mathrm{d}^{j+k}I(x)}{\mathrm{d}x^{j+k}}A_j + \left[\dfrac{\mathrm{d}^{2k}I(x)}{\mathrm{d}x^{2k}} - \delta_{k3}\dfrac{\rho U}{L}\dfrac{\partial^k\xi(x,0;0)}{\partial x^k}\right]A_k = \displaystyle\int_{S_B}\left[\phi\frac{\partial^{k+1}\xi}{\partial x^k\partial n_0} - \frac{\partial^k\xi}{\partial x^k}\frac{\partial\phi}{\partial n_0}\right]\mathrm{d}s_0\end{cases}, \quad x\to 0^{\pm}. \tag{16}$$

In Eq. (16), the integrand of $I(x)$ is of $O(\alpha^{-4})$ as $|\alpha|\to+\infty$. Hence, $\mathrm{d}^n I(x)/\mathrm{d}x^n$ is fully convergent when $n\le 2$. When $n = 3\sim5$, the terms associated with the Dirac delta function $\delta(x)$ can be extracted from the integral. It should be noted that $\mathrm{d}^6 I(x)/\mathrm{d}x^n$ is divergent, but the combination

$$\frac{\mathrm{d}^6 I(x)}{\mathrm{d}x^6} - \frac{\rho U}{L}\frac{\partial^3\xi(x,0;0)}{\partial x^3} = -\frac{2\pi\rho}{L}\delta''(x) - \frac{\rho^2 g}{L}\int_{-\infty}^{+\infty}\frac{\alpha^3\sinh(\alpha H)}{K(\alpha,U)}e^{-\mathrm{i}\alpha x}\mathrm{d}\alpha \tag{17}$$

leads to a convergent result. In such a case, for a given edge, once A_j and A_k are solved from Eq. (16), Eq. (11) can be solved using the BEM for a submerged body [6]. In the specific case of a circular cylinder, the solution can be solved using the multipole expansion [4, 5], based on the Green function satisfying the constraint condition, which can be derived following a procedure similar to that in [8]. In fact, we can eliminate A_j and A_k from Eq. (11) using (16). This becomes an integral equation over S_B only with the Green function satisfying the constraint conditions.

Once the solution is found, the resistance F_R and lift F_L on the body can then be found using

$$F_L - \mathrm{i}F_R = \int_{S_B} p(n_z + \mathrm{i}n_x)\mathrm{d}s, \tag{18}$$

where the hydrodynamic pressure p can be calculated from the Bernoulli equation

$$p = \frac{1}{2}\rho\nabla(\phi - Ux)\cdot\nabla(\phi - Ux). \tag{19}$$

3 RESULTS AND DISCUSSION

Case studies are made of a circular cylinder. Numerical results are nondimensionalised based on the density of water ρ, acceleration due to gravity g and cylinder radius a. The following typical parameters are used, $L/\rho g a^4 = 72.9319$, $H/a = 8$, $h/a = 0.2$ and $z_c/a = -2$. The critical Froude number [5] is at $F_c \approx 0.7869$. Four different transverse positions are considered, and a clamped constraint is imposed at $x = 0$. The hydrodynamic forces against F are shown in Figure. 2. It is observed that the x_0/a has a significant influence on F_R and F_L, particularly when F is near $F = F_c$ or $F = 1$. Taking the case of $x_0/a = 4$ as an example, the profiles of ice sheet deflections

at three different regimes of Froude numbers are presented in Figure. 3, where the wave patterns at different F are clearly illustrated.

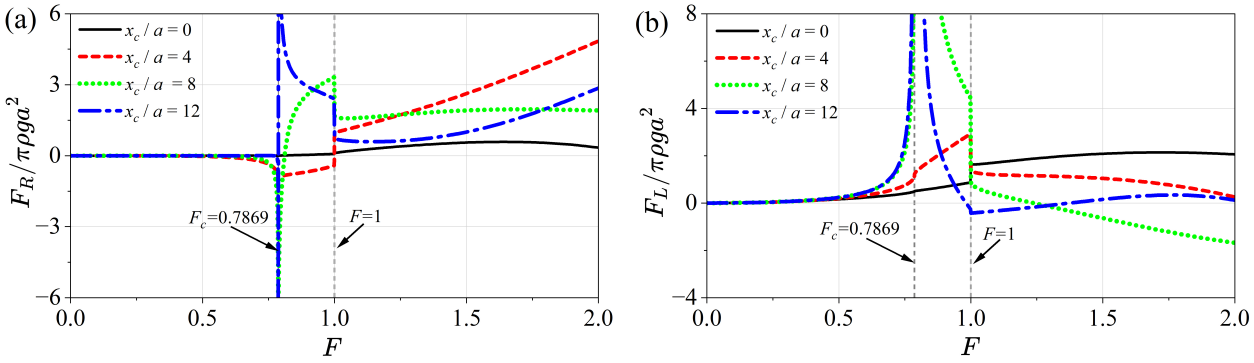

Figure. 2. Forces on a circular cylinder against F at four different transverse positions. (a) Resistant; (b) Lift; (clamped constraint is imposed at $x = 0$)

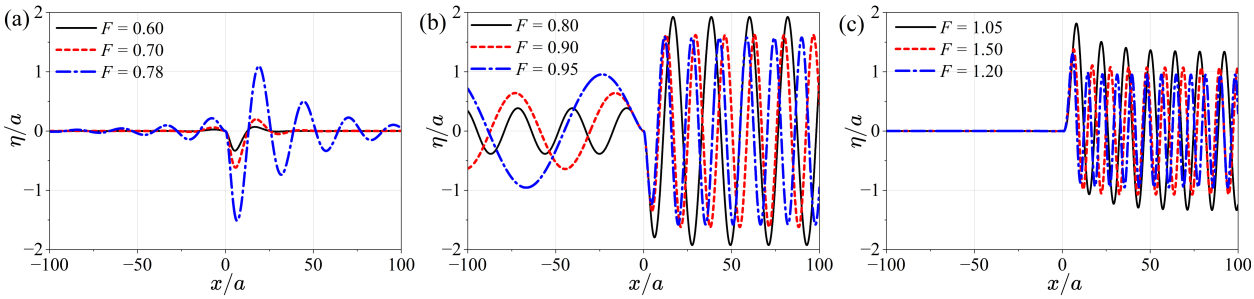

Figure. 3. Ice sheet deflection at different regions of the Froude number. (a) $0 < F < F_c$; (b) $F_c < F < 1$; (c) $F > 1$. ($x_0/a = 4$, clamped constraint is imposed at $x = 0$)

4 CONCLUSIONS

The interaction of a uniform current with a cylinder submerged below a homogeneous ice sheet with an internal constraint is considered, and solutions for clamped, simply supported, and free edge conditions are presented. Numerical results for hydrodynamic forces and profiles of ice sheet deflection at the clamped edge are shown and analysed. Results for other cases and their physical significance will be provided and discussed in the workshop.

REFERENCES

[1] Kozin, V. M., & Onishchuk, A. V., 1994. Model investigations of wave formation in solid ice cover from the motion of a submarine. *Journal of applied mechanics and technical physics*, *35*(2), 235-238.

[2] Savin, A. A., & Savin, A. S., 2012. Ice cover perturbation by a dipole in motion within a liquid. *Fluid Dynamics*, *47*(2), 139-146.

[3] Sturova, I. V., 2013. Unsteady three-dimensional sources in deep water with an elastic cover and their applications. *Journal of Fluid Mechanics*, *730*, 392-418.

[4] Li, Z. F., Wu, G. X., & Shi, Y. Y., 2019. Interaction of uniform current with a circular cylinder submerged below an ice sheet. *Applied Ocean Research*, 86, 310-319.

[5] Yang, Y. F., Wu, G. X., & Ren, K. 2024. Interaction between a uniform current and a submerged cylinder in a marginal ice zone. Journal of Fluid Mechanics, 984, A50.

[6] Yang, Y. F., & Wu, G. X. 2025. A uniform current passing bodies submerged beneath an ice sheet at critical Froude numbers. Journal of Fluid Mechanics, 1018, A45.

[7] Timoshenko, S. P. & Woinowsky, K. S., 1959. *Theory of Plates and Shells.* McGraw-Hill.

[8] Li, Z. F., Wu, G. X., & Ji, C. Y. 2018. Wave radiation and diffraction by a circular cylinder submerged below an ice sheet with a crack. *Journal of Fluid Mechanics*, *845*, 682-712.